orpk mouse model of polycystic kidney disease reveals essential role of primary cilia in pancreatic tissue organization

David A. Cano[1], Noel S. Murcia[2], Gregory J. Pazour[3] and Matthias Hebrok[1,*]

[1]Diabetes Center, Department of Medicine, University of California, San Francisco, CA 94143, USA
[2]Department of Pediatrics, Case Western Reserve University, Cleveland, OH 44106, USA
[3]Program in Molecular Medicine, University of Massachusetts Medical School, Worcester, MA 01605, USA
*Author for correspondence (e-mail: mhebrok@diabetes.ucsf.edu)

Accepted 29 March 2004

Development 131, 3457-3467
Published by The Company of Biologists 2004
doi:10.1242/dev.01189

Summary

Polycystic kidney disease (PKD) includes a group of disorders that are characterized by the presence of cysts in the kidney and other organs, including the pancreas. Here we show that in *orpk* mice, a model system for PKD that harbors a mutation in the gene that encodes the polaris protein, pancreatic defects start to occur at the end of gestation, with an initial expansion of the developing pancreatic ducts. Ductal dilation continues rapidly after birth and results in the formation of large, interconnected cysts. Expansion of pancreatic ducts is accompanied by apoptosis of neighboring acinar cells, whereas endocrine cell differentiation and islet formation appears to be unaffected. Polaris has been shown to co-localize with primary cilia, and these structures have been implicated in the formation of renal cysts. In the *orpk* pancreas, cilia numbers are reduced and cilia length is decreased. Expression of polycystin-2, a protein involved in PKD, is mislocalized in *orpk* mice. Furthermore, the cellular localization of β-catenin, a protein involved in cell adhesion and Wnt signaling, is altered. Thus, polaris and primary cilia function are required for the maturation and maintenance of proper tissue organization in the pancreas.

Key words: Pancreas, Cilia, Polycystic kidney disease, Polaris, *orpk*, Acinar-ductal metaplasia, Wnt signaling

Introduction

Polycystic kidney disease (PKD) includes a group of autosomal dominant (ADPKD) and autosomal recessive (ARPKD) disorders characterized by the presence of cysts in the kidney and other organs, such as liver (50% frequency) and pancreas (10% frequency) (see Calvet and Grantham, 2001; Gabow, 1993; Igarashi and Somlo, 2002; Murcia et al., 1999; Wilson, 2001). ADPKD, the most common form (incidence of 1 in 1000 adults) is usually caused by defects in the *Pkd1* and *Pkd2* genes. ARPKD is less frequent (incidence of 1 in 10,000 live births) and is commonly caused by defects in the *Pkhd1* gene (Igarashi and Somlo, 2002). In mice, typical pathologies of PKD are found in animals carrying mutations in the *Pkd1* and *Pkd2* (Lu et al., 2001; Wu et al., 2000), *cpk* (*Cys1* – Mouse Genome Informatics) (Ricker et al., 2000), *bpk* (*Bicc1* – Mouse Genome Informatics) (Nauta et al., 1993), inversin (Morgan et al., 1998) and *Tg737* genes (Moyer et al., 1994).

Recent observations have indicated that primary cilia, cellular appendages that are present on the surface of most cells (Wheatley et al., 1996), play a crucial role during the development of PKD (Ong and Wheatley, 2003). *Tg737*, the gene mutated in the *orpk* mouse model of PKD encodes polaris, a protein required for proper ciliary assembly (Pazour et al., 2000; Taulman et al., 2001; Yoder et al., 2002b). Furthermore, both polycystin-1 and polycystin-2, the proteins encoded by *Pkd1* and *Pkd2*, respectively, localize to the cilium in mouse and human kidney cells (Pazour et al., 2002; Yoder et al., 2002a). In addition, the genes mutated in the *cpk* and inversin PKD mouse models encode the proteins cystin and inversin, respectively, which also localize to the cilia (Hou et al., 2002; Watanabe et al., 2003). Finally, Lin et al. have shown that the kidney-specific inactivation of kinesin-II, a protein essential for cilia formation, leads to PKD in mice (Lin et al., 2003). Thus, increasing evidence points to defects in cilia assembly and function as a cause of PKD.

Although numerous studies have focused on the renal pathologies, less attention has been paid to the extrarenal abnormalities. Here, we present a detailed study of the pancreatic defects in one of the PKD models, the *orpk* mouse. Our findings show that a mutation in the *Tg737* gene results in severe abnormalities in the pancreas, including massive acinar cell loss, formation of abnormal tubular structures, and appearance of endocrine cells in ducts. We demonstrate that pancreatic cells in *orpk* mice are marked by a reduction in cilia number and aberrant cilia architecture, which suggests that the pancreatic defects are caused by improper cilia assembly. We find similar pancreatic abnormalities in mice carrying mutations in the *Pkd2* and inversin genes. Both Pkd2 and inversin proteins localize to cilia and mediate cilia function; however, in contrast to the orpk/polaris protein, they are not required for cilia formation. These observations indicate that both accurate cilia assembly and function are essential for maintenance of proper pancreatic tissue organization. Cell signaling properties of ductal cells are affected, as mislocalization of β-catenin and increased expression of transcriptional activators of Wnt signaling are observed in

orpk mice. Thus, our results suggest that pancreatic PKD phenotypes are at least in part mediated through the deregulation of Wnt signaling activity.

Materials and methods

Mice

Mice used in these studies were maintained in the barrier facility according to protocols approved by the Committee on Animal Research at the University of California, San Francisco. *Tg737^{orpk}* (*orpk*), *Tg737$^{\Delta 2\text{-}3\beta gal}$*, inversin and *Pkd2* mice have been described previously (Morgan et al., 1998; Moyer et al., 1994; Murcia et al., 2000; Wu et al., 2000).

Tissue preparation, immunohistochemistry and microscopy

Isolated pancreata from E12.5, E15.5 and E18.5 embryos, newborn and adult mice were fixed in 4% (w/v) paraformaldehyde (PFA) in phosphate-buffered saline (PBS) for 1 to 4 hours at 4°C. Histological analysis, quantification of the tissue area and counting of cells, were performed as described previously (Hebrok et al., 2000). Hematoxylin/Eosin staining, immunohistochemical and immunofluorescence analyses were performed on paraffin sections as described previously (Kim et al., 1997). The following primary antibodies were used: guinea pig anti-insulin, diluted 1:500 (Linco); rabbit anti-glucagon, diluted 1:500 (Linco); rabbit anti-Pdx1, diluted 1:3000 (gift from Dr Michael German); rabbit anti-Glut2, diluted 1:1000 (Chemicon); rabbit anti-amylase, diluted 1:700 (Sigma); rabbit anti-cleaved caspase 3, diluted 1:100 (Cell Signaling Technology); anti-Pkd2, diluted 1:1000 (Cai et al., 1999) (G.J.P., unpublished); anti-acetylated tubulin 611b1, diluted 1:10,000 (Sigma); mouse anti-β-catenin, diluted 1:100 (BD Biosciences); rabbit anti-Ki-67, diluted 1:200 (Novocastra Laboratories); and Armenian hamster anti-Muc1, diluted 1:200 (Neomarkers).

The following secondary antibodies were used for immunofluorescence: FITC-conjugated anti-guinea pig (Molecular Probes); Cy3-conjugated anti-rabbit (Molecular Probes); FITC-conjugated anti-Armenian hamster (Jackson ImmunoResearch); Alexa488-congugated anti-rabbit; and Alexa594- or Alexa693-conjugated anti-mouse (Molecular Probes). Fluorescence was visualized and photographed with a Zeiss Axiphoto2 plus and a Leica TCS SP2 confocal microscope.

Terminal transferase-mediated dUTP nick end labeling (TUNEL) analysis

Immunohistochemical analysis for apoptosis was performed following the manufacturer's recommendations (Invitrogen). In brief, the sections were deparaffinized, rehydrated in graded alcohols and incubated with 20 μg/ml proteinase K for 2 minutes. They were then incubated with 3% hydrogen peroxide in methanol for 30 minutes to inactivate endogenous peroxidase, and treated with terminal deoxynucleotidyl transferase and digoxigeniuridine triphosphate (dUTP) for 60 minutes at 37°C. To visualize the nick-end labeling with a light microscope, the sections were treated with anti-digoxigenin HRP conjugate (Roche) for 30 minutes and then incubated with diaminobenzidine-tetrahydrochloride (Vector). Apoptosis was quantified by averaging the number of stained nuclei per field.

Staining for β-galactosidase activity

Pancreata isolated from heterozygous *Tg737$^{\Delta 2\text{-}3\beta gal}$* mutant mice, in which the *lacZ* gene was inserted into the *Tg737* locus (Murcia et al., 2000), were fixed for 4 hours at 4°C in 4% paraformaldehyde and then incubated overnight in phosphate-buffered saline (PBS) supplemented with 5-bromo-4-chloro-3-indolyl-D-galactopyranoside (X-gal; 400 μg/ml) at 4°C. The dissected organs were photographed on a Leica MZ FL3 equipped with a Leica IM500 system.

Morphometric quantification of islet areas

Morphometric analysis was performed as described previously (Hebrok et al., 2000). In short, a portion of the whole pancreas was used for quantification to obtain representative results. The first five consecutive sections of P9 pancreatic tissue were mounted on the first of a series of microscope slides, followed by the next five sections placed on the second slide. A total of five individual slides (1a-5a) were filled with consecutive sections. When necessary, additional series of five (1b-5b, etc.) slides were prepared until all pancreatic sections were mounted. After immunohistochemistry, pancreatic epithelial areas were outlined and measured with the OpenLab software. Insulin- and glucagon-positive areas of the P9 pancreas were measured on every twenty-fifth section (every 150 μm) from one set of slides (1a-1e). Data analysis was performed with Excel software (Microsoft). Statistical significance was assessed by employing the Student's *t*-test.

Quantification of cilia length

Immunofluorescent images of cilia stained for acetylated tubulin were acquired using a Leica TCS SP2 confocal microscopy system with Leica Confocal Software (LCS). Images were acquired in 50 confocal z-stack slices and composite images were prepared using LCS, from which μm measurements of cilia length were obtained. Data analysis was performed with Excel software.

RNA preparation and RT-PCR analysis

Dissected pancreata were dissolved in Trizol (Gibco-BRL) and total RNA was prepared according to the manufacturer's instructions. RT-PCR was performed as described in Wilson and Melton (Wilson and Melton, 1994). PCR was performed under the following conditions: 1 cycle of 95°C for 10 minutes; followed by 35 cycles of 94°C for 45 seconds, 60°C for 45 seconds and 72°C for 1 minute. Mouse actin was used as the internal control. Initial experiments were carried out to ensure that conditions for PCR were within the linear range of amplification.

Expression of Lef1, Tcf1, Tcf3, and Tcf4 mRNA in P11 pancreata was studied by RT-PCR. Primers were designed to span introns to exclude nonspecific genomic DNA amplification. Forward and reverse primer sequences used are listed 5′ to 3′. Primers used were:

Lef1, ACA GTG ACC TAA TGC ACG TGA AGC C and CGC TGA CCA GCC TGG ATA AAG CT;

Tcf1, GAA GCC AGT CAT CAA GAA ACC CCT C and TGT TTT TCC CTT GAC CGC CTC TTC;

Tcf3, GAG AAG CCT TGT GAT AGC CCT GCG and AAG TAG GGG GAG AGG TCA GCA GAG C;

Tcf4, 5′AGA GCG AAG GTG GTG GCC GAA T; and

actin, ATG ACG ATA TCG CTG CGC TGG T and ATA GGA GTC CTT CTG ACC CAT TCC.

Results

Pancreatic abnormalities in *Tg737^{orpk}* mice

Tg737^{orpk} (hereafter *orpk*) homozygous mutant mice exhibit a pleiotropic phenotype that includes cystic kidneys and liver, skeletal abnormalities and pancreatic defects. The severity of these defects results in early postnatal lethality with homozygous mutants rarely surviving beyond the second week after birth (Moyer et al., 1994). To test whether morphological changes in pancreas formation occur postnatally or are initiated during embryonic development, we have characterized the pancreatic defects displayed by *orpk* mice through developmental and postnatal stages.

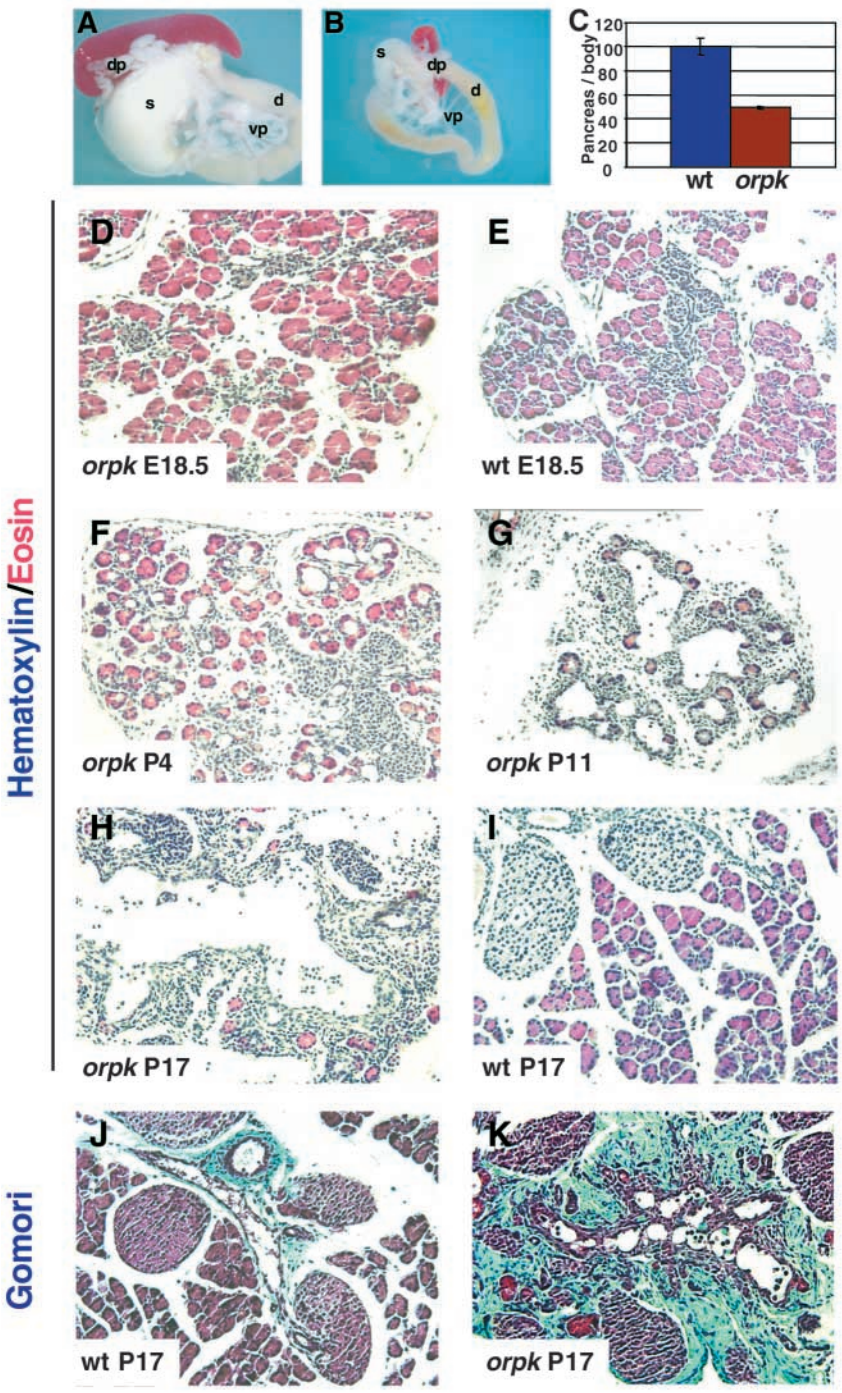

Fig. 1. Defects in pancreas maturation in *orpk* mice. Pancreatic mass is reduced in *orpk* mice (B) when compared with wild type (A) at P9. To adjust for differences in body mass, pancreas weight was divided by body weight (C; blue, wild type, *n*=5; red, *orpk*, *n*=5). Progressive acinar cell loss and ductular hyperplasia increase in *orpk* mice with age (D,F-H) when compared with wild type (E,I). Gomori trichrome staining reveals a significant increase in collagen deposition in *orpk* pancreas (K) when compared with wild-type tissue (J). d, duodenum; dp, dorsal pancreas; s, stomach; vp, ventral pancreas.

Analysis of Hematoxylin/Eosin-stained tissue did not reveal major changes in pancreas gross morphology at the end of gestation (Fig. 1D,E; changes in embryonic cell differentiation and morphology are discussed below). After birth, a progressive loss of exocrine cells, accompanied by increased dilation of duct-like structures, was observed in postnatal day 0 (P0) to P17 mice (Fig. 1F-I). The acinar architecture was poorly organized, marked by the loss of the typical round shape of the acini and the presence of duct-like structures composed of cuboidal cells. The substantial decrease in acinar tissue results in a severe reduction of total pancreatic mass, even when the reduced body size of the mutants is taken into account (Fig. 1A-C). These defects might contribute to the overall smaller size of the *orpk* mice by limiting their digestive capability.

The wild-type pancreas consists of distinct lobules that are connected via interlobular ducts. In *orpk* mice, pancreatic lobules are separated by an expansion of the interstitial space, as well as by an increased number of tubular complexes and mesenchymal stroma within individual lobules (Fig. 1F-I). Two weeks after birth, few residual acini were present and large ductal cysts had formed (Fig. 1H-I). Cellular debris was found within the lumen of these large cysts, indicating the occurrence of massive cell death within pancreatic tissue (Fig. 1F-I, Fig. 4A-B). Gomori trichrome staining revealed a substantial increase in collagen deposition throughout the organ, suggesting elevated levels of mesenchymal stroma (Fig. 1J,K). In contrast to wild-type pancreas, where stromal cells normally surround large interlobular ducts and blood vessels, these cells were found throughout the pancreas in the *orpk* mice. Thus, polaris, the protein encoded by the *Tg737* gene, is essential for maturation of pancreatic tissue organization after birth. No obvious phenotypes were observed in the pancreata of *orpk* heterozygous mice (data not shown), a finding that supports previous studies reporting the analysis of other organs (Moyer et al., 1994).

Tg737 expression in pancreatic tissue

Although *Tg737* expression had been demonstrated in several other tissues (Taulman et al., 2001), expression within the pancreas has not been reported. Here we analyzed the *Tg737* expression pattern in pancreatic tissue at different developmental stages by monitoring β-galactosidase activity in previously generated $Tg737^{\Delta 2\text{-}3\beta gal}$ knockout mice in which the *lacZ* gene is expressed under control of endogenous promoter in mice (Murcia et al., 2000). At E15.5, β-galactosidase activity/*Tg737* expression was detected throughout the pancreatic tissue in a punctate pattern (Fig. 2A). Although the basis for this punctate pattern is unknown, similar β-galactosidase patterns have been previously described for other cell types expressing *Tg737* (Nakanishi et al., 2001;

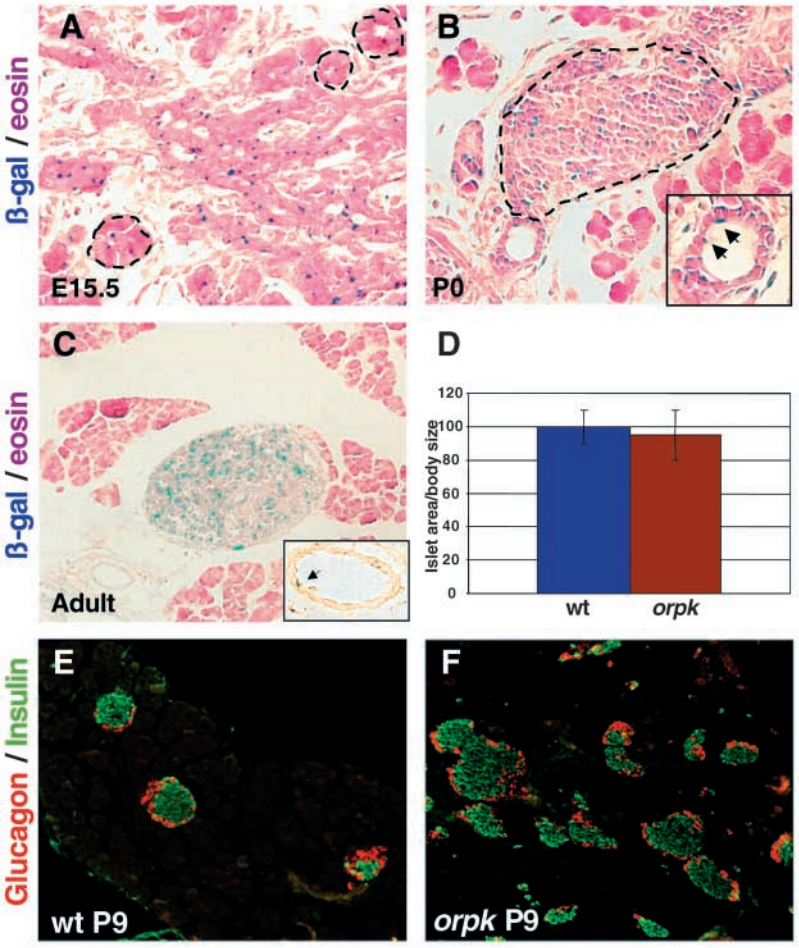

Fig. 2. *Tg737* expression in pancreatic tissue and islet formation in *orpk* mice. Staining for β-galactosidase activity in heterozygous *Tg737* mice that carry the *lacZ* gene under control of the endogenous *Tg737* promoter reveals broad expression in the pancreas at E15.5 (A). Expression becomes progressively confined to islets and intercalated ducts in newborn (B) and adult animals (C). Insets in B and C show expression in ductal cells (arrows). Acini in A and islets in B are outlined for a better visualization. Islet formation is unaffected in *orpk* mice (E,F). Islets were stained with antibodies directed against centrally located insulin (green) and marginally located glucagon-producing cells (red). Quantification of islet areas revealed no difference between wild-type and *orpk* mice at P9 (D). To adjust for differences in body mass, islet area was divided by body weight. (D; blue, wild type, *n*=5; red, *orpk*, *n*=5). Wild-type islet area was adjusted to '1' to facilitate comparison. Errors bars are shown as ±s.e.m.

Taulman et al., 2001). Within forming acini, *Tg737* expression was confined to the luminal side, a pattern that precludes determining whether the staining is confined to acinar or centro-acinar cells (a ductal cell type; Fig. 2A). After birth, *Tg737* expression remained high in islets and intercalated ducts, but was not detected in intracinar ducts (Fig. 2B). In adult tissues, the *Tg737* expression pattern was similar to that observed in newborn animals; however, only a subset of cells in the intercalated ducts were marked by β-galactosidase activity (Fig. 2C).

Endocrine tissue is unaffected in *orpk* mice

The highest *Tg737* expression levels were found in endocrine islet cells, raising the possibility that endocrine cell development and islet formation was altered in *orpk* mice. Histological analysis of Hematoxylin/Eosin-stained pancreatic sections indicated that the islets have normal architecture (Fig. 1F). This was supported by the results of the immunofluorescent staining of islets with antibodies directed against insulin and glucagon. A central core of insulin-producing β-cells surrounded by glucagon-positive α-cells was detected in both mutant and wild-type pancreas (Fig. 2E,F). No differences in the expression of mature β-cell markers, including the transcription factor pancreatic and duodenal homeobox gene 1 (Pdx1) and glucose transporter 2 (Glut2), a low-affinity transporter present in the plasma membrane of pancreatic β-cells, were observed in *orpk* mice (data not shown). Furthermore, morphometric analysis revealed no differences in the overall islet area when compared with wild-type mice (Fig. 2D). The only difference observed was an apparent clustering of islets in *orpk* pancreata (Fig. 2E,F) that could be explained by the reduction in overall pancreas size due to the profound loss of acinar cells. Thus, in spite of the high levels of *Tg737* expression observed in islet cells, polaris protein is not essential for β-cell differentiation and islet formation.

The early lethality and compromised health of *orpk* mice prohibited any physiological assays to determine whether cilia are necessary for mature β-cell function. Glucose tolerance tests performed in heterozygous adult *orpk* mice revealed no differences compared with wild-type littermates (data not shown).

Acinar cell loss and expansion of duct-like epithelium in newborn *orpk* mice

Although the endocrine compartment appears to form normally, significant loss of acinar tissue was observed in *orpk* mice (Fig. 1F-I). The exocrine portion of the pancreas is organized as a tubuloalveolar gland. Acini secrete digestive enzymes into intracinar ducts that conduct to progressively larger intercalated ducts, interlobular ducts and eventually to the main pancreatic duct. To further characterize the exocrine defects, we performed immunofluorescent staining with antibodies directed against amylase, a digestive enzyme produced by acinar cells. At the end of gestation, E18.5 *orpk* embryos showed normal amylase staining (Fig. 3A,B). However, shortly after birth, amylase expression was significantly reduced throughout the exocrine tissue in *orpk* mice (Fig. 3C-F). Concomitant with the progressive loss of acinar cells, we observed an increase in ductal structures in pancreatic sections when stained with antibodies directed against mucin 1 (Muc1), a membrane protein expressed in epithelial cells lining glands and ducts in several organs (Graham et al., 2001). In wild-type pancreas the Muc1 antibody specifically labeled all cells of the ductal system, including intracinar ducts and intercalated ducts. No cross reactivity with blood vessels or any other cells type was

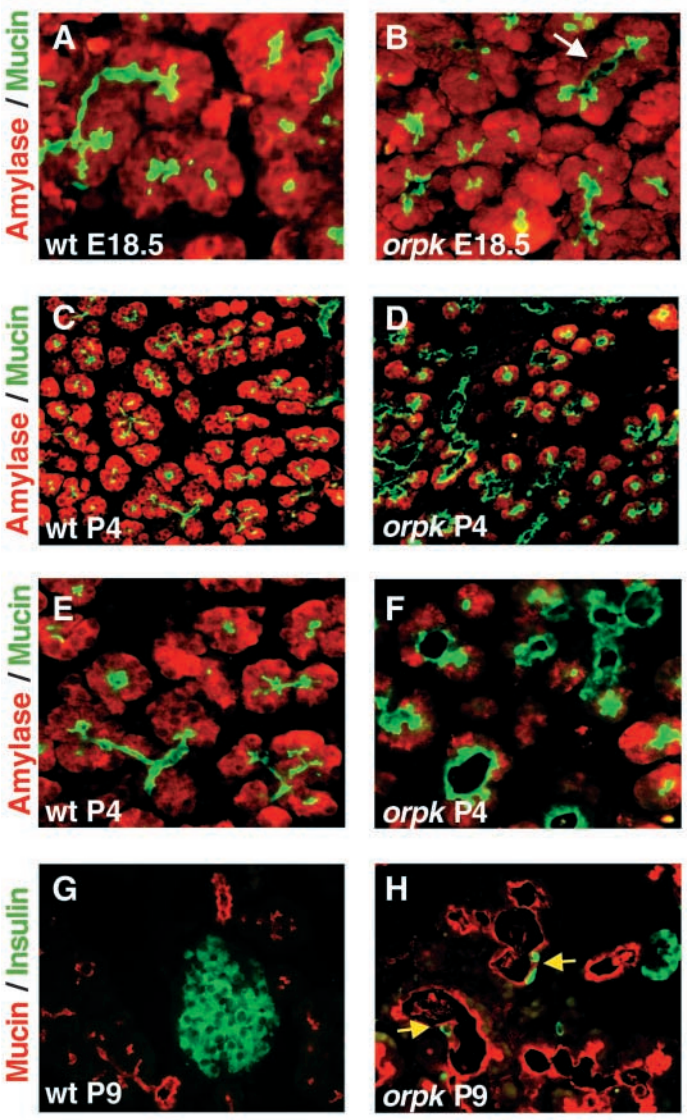

Fig. 3. Acinar cell loss and ductular hyperplasia in *orpk* mice. Staining for amylase indicates normal exocrine architecture in E18.5 *orpk* pancreatic tissue (A,B). Mucin 1 staining reveals ductal defects in *orpk* mice with small dilations of intracinar ducts (arrow in B). After birth (P4), extensive acinar cell loss occurs, as shown by the decrease of amylase staining in *orpk* mice (C,D; shown at higher magnification in E,F). Increased dilation of duct-like structures was observed after birth (P4), as shown by mucin staining (C-F). Insulin-expressing cells are present in duct-like structures of *orpk* mice at P9 (H, arrows). No insulin-expressing cells could be detected in ducts of wild-type mice at P9 (G).

observed with the antibody (Fig. 3). By employing this cell specific marker, we were able to detect defects in ductal morphology in *orpk* pancreata starting at E18.5, with intracinar ducts displaying small dilations not typically observed in wild-type pancreas (Fig. 3A,B). Associated with a reduction of amylase immunoreactivity, we detected a rapid expansion of pancreatic ducts in mutant tissue after birth (Fig. 3C-F). Interestingly, insulin-expressing cells were frequently detected in the expanding duct-like structures (Fig. 3H) soon after birth. These insulin-positive cells also expressed mature β-cell markers, including Pdx1 and glucose transporter 2 (Glut2) (data not shown). At the stages analyzed, we failed to detect any insulin-expressing cells in ducts of wild-type pancreas (Fig. 3G).

Loss of exocrine tissue is caused by increased acinar cell apoptosis

A growing body of evidence suggests that apoptosis plays a major role during PKD formation in human, mice and rat (Ali et al., 2000; Ecder et al., 2002; Lanoix et al., 1996; Saadi-Kheddouci et al., 2001; Sorenson et al., 1996; Trudel et al., 1997; Woo, 1995). Furthermore, elevated levels of several pro-apoptotic genes have been reported in pancreatic tissue in *cpk* mice, another model of PKD (Gattone et al., 2002). TUNEL analysis revealed a sixfold increase in apoptotic cells in *orpk* pancreatic tissue when compared with wild-type tissue (Fig. 4A,B,E). The majority of TUNEL-positive cells were found outside of the duct-like epithelium, suggesting selective apoptosis of acinar cells. Staining with antibodies directed against the active form of caspase 3 showed that the caspase pathway is induced during acinar cell apoptosis in *orpk* mice (data not shown). By contrast, no apoptotic cells were detected in the islets (Fig. 4B, inset).

Increased proliferation of duct-like cells

One of the hallmarks of PKD is the abnormal proliferation of immature epithelial cells (Gabow, 1993; Murcia et al., 1999). To test whether the expansion of the duct-like epithelium in *orpk* mice is due to an increase in cell proliferation, we counted cells marked by the expression of Ki-67, a nuclear non-histone protein present only in cells progressing through the cell cycle. Ki-67-positive cells were detected in endocrine, acinar and ductal tissue, with the highest levels found in expanding ducts of *orpk* mice (Fig. 4C,D). Measurement of the proliferation indexes, defined as the number of Ki-67-positive cells per field, revealed reduced proliferation of acinar cells and β-cells in *orpk* mice (Fig. 4F). By contrast, *orpk* ductal cells showed a proliferation index similar to that found in wild-type animals, resulting in a 3-fold relative increase of ductal cell proliferation when compared with *orpk* acinar and β-cells (Fig. 4F). This is in stark contrast with control animals in which only a small difference was detected in proliferation indexes between acinar/β-cells and ductal cells (1.4 fold). Thus, *orpk* ductal cells are marked by a relative increase in proliferation compared with other pancreatic cell types, a defect that results in duct expansion and formation of large pancreatic cysts.

Impaired cilia formation in pancreatic cells of *orpk* mice

The murine *Tg737* gene (and its homologs in the algae *Chlamydomonas* and the worm *C. elegans*) is involved in primary cilia formation (Pazour et al., 2000). Several of the phenotypes associated with mutations in *Tg737*, such as polycystic kidney disease, defects in left-right patterning and retinal degeneration are associated with ciliary assembly defects in these tissues (Murcia et al., 2000; Pazour et al., 2000; Pazour et al., 2002; Yoder et al., 2002b). As *Tg737* expression is detected in all pancreatic cell types known to express cilia (Aughsteen, 2001), we wanted to know whether pancreatic cells in *orpk* mice displayed primary cilia defects. To determine the effects of the *orpk* mutation on the formation of pancreatic

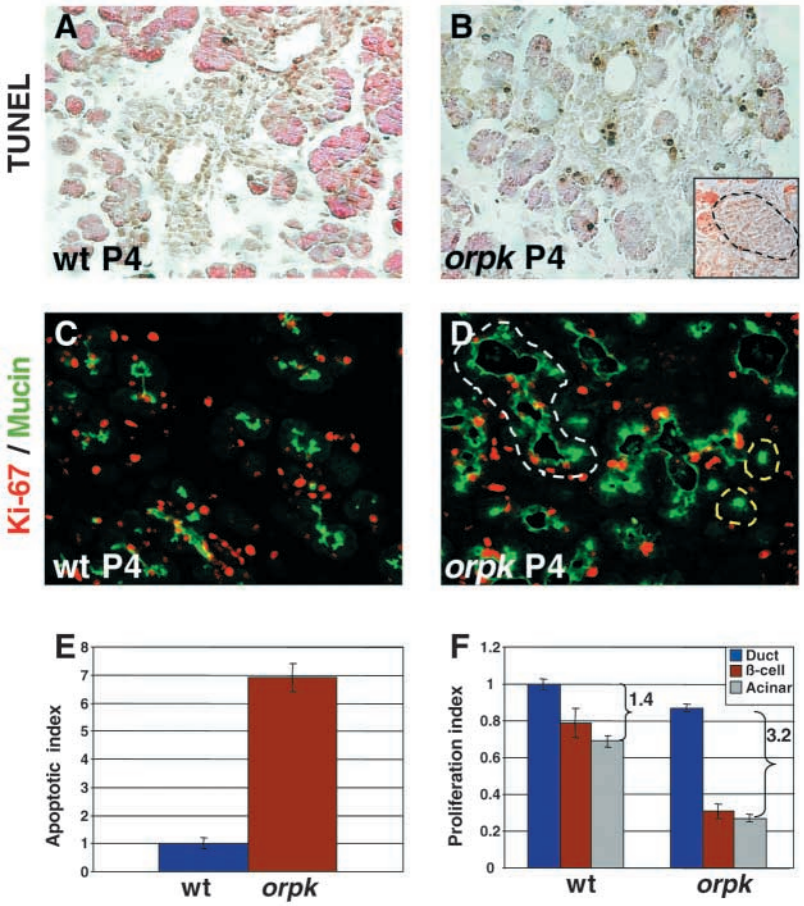

Fig. 4. Increase of acinar cell apoptosis and ductal proliferation in *orpk* mice after birth (P4). TUNEL staining showed an increase of apoptotic cells in pancreas of *orpk* mice (B) when compared with wild-type mice (A). Inset in B shows that no apoptotic cells could be detected in islets (outlined) in *orpk* mice. Proliferation is increased in dilated ducts of *orpk* mice, as shown by Ki-67 staining (C,D). Note that the number of proliferating cells in *orpk* mice in dilated ducts (outlined in white) is higher than in non-dilated ducts (outlined in yellow). Quantification of apoptotic cells, measured as number of cells positive for TUNEL staining per field of view (E; blue, wild type, *n*=5; red *orpk*, *n*=5), showed an increase of cell apoptosis in *orpk* mice. Proliferation indexes of pancreatic cells are given as number of Ki-67-positive cells per mucin-positive, insulin-positive or amylase-positive cells (F; wild type, *n*=5; *orpk*, *n*=5). Wild-type numbers for apoptosis and proliferation were set to '1' to facilitate comparison (E,F). Errors bars are shown as ±s.e.m.

cilia, pancreatic sections were stained with an antibody directed against acetylated tubulin, a protein that is preferentially localized in the ciliary axoneme. In wild-type pancreas, primary cilia were present in tissues marked by $Tg737^{\Delta 2\text{-}3\beta gal}$ expression, including the luminal surface of cells in interlobular, intercalated and intracinar ducts, and in islets (Fig. 2, Fig. 5A,C,E). During embryonic development primary cilia were found throughout the pancreatic epithelium as early as E12.5 (data not shown). By contrast, primary cilia were almost absent in *orpk* pancreata at all stages analyzed (Fig. 5B,D,F). Morphometric quantification of cilia lengths using confocal microscopy at E15.5, E18.5 and P4 revealed that the remaining primary cilia in pancreatic cells of *orpk* mice are significantly shortened when compared with wild-type primary cilia (Fig. 5G). The observation that cilia length is already reduced in E15.5 pancreatic tissue, in addition to the observed changes in duct morphology at E18.5 (Fig. 3A,B), further supports the hypothesis that pancreatic deficiencies in *orpk* mice result from embryonic defects. Furthermore, these results indicate that polaris is required for proper assembly of primary cilia in pancreatic cells.

Increased polycystin-2 expression in duct-like epithelium

Pkd1 and *Pkd2* are linked to the most common forms of autosomal dominant polycystic kidney disease (Igarashi and Somlo, 2002). Interestingly, the protein encoded by the *Pkd2* gene, polycystin-2, localizes to renal cilia (Pazour et al., 2002) and polycystin-2 expression levels are increased in the shortened primary renal cilia of *orpk* mice (Pazour et al., 2002). To determine whether a similar mislocalization of polycystin-2 could be observed in pancreatic cells of *orpk* mice, we stained sections of mutant and wild-type pancreas with polycystin-2 antibodies. This staining revealed polycystin-2 expression in interlobular and intercalated ducts, a pattern similar to that previously described for polycystin-1 and polycystin-2 in human pancreas (Fig. 5A) (Foggensteiner et al., 2000; Geng et al., 1996; Ong et al., 1999). Expression of polycystin-2 was increased in *orpk* pancreas. All dilated intracinar ducts showed high polycystin-2 expression, comparable to levels that were observed only in intercalated ducts of control mice (Fig. 5A,B). Furthermore, subcellular localization of polycystin-2 in pancreatic cells of *orpk* mice is somewhat different than what was previously observed in kidney collecting tubules of *orpk* mice. Whereas the increase in polycystin-2 in *orpk* kidney cells is confined to the cilia (Pazour et al., 2002), a general increase was observed throughout the cytoplasm of pancreatic *orpk* cells, with highest concentrations found near the plasma membrane along both the apical and basolateral membranes (Fig. 5B). Although the difference between polycystin-2 protein localization in *orpk* kidney and pancreatic cells might present an unexplored tissue-specific phenomenon, these results suggest a connection between defective cilia assembly and duct dilation.

Pancreatic abnormalities in inversin and *Pkd2* mice

The observation that *orpk* mutants showed increased polycystin-2 localization in dilated ducts could suggest that defective cilia function, as a consequence of impaired cilia formation, is responsible for the observed pancreatic abnormalities. To determine whether ciliary dysfunction causes similar pancreatic phenotypes, we decided to characterize pancreas morphology in other PKD mouse models harboring mutations in the inversin and *Pkd2* genes. Although both genes encode proteins known to localize in the cilia of kidney cells,

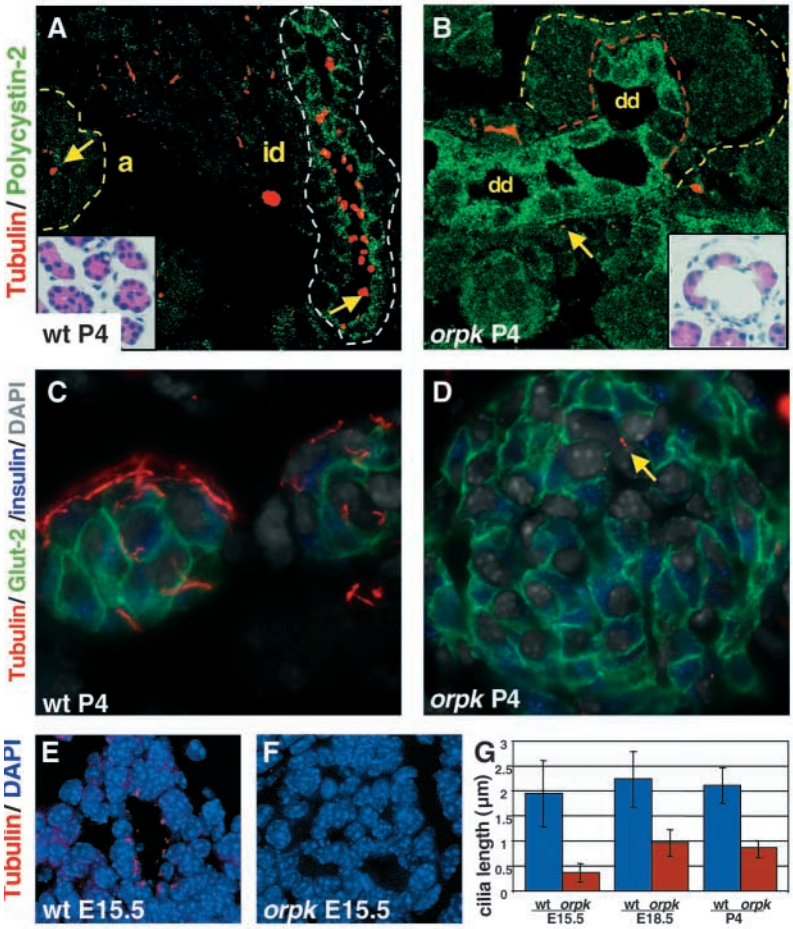

Fig. 5. Absence of pancreatic cilia and increased polycystin-2 expression in *orpk* mice. In wild-type pancreatic sections (A) polycystin-2 expression is localized in intercalated ducts. Cilia were visualized using an antibody against acetylated tubulin. Cilia are confined to the lumen of intracinar and intercalated ducts (arrows). Acini (a) and intercalated ducts (id) are outlined in yellow and white, respectively, for better visualization. Inset shows Hematoxylin/Eosin staining of acini in wild type. A dramatic decrease in cilia number is detected in *orpk* mice (B; arrow). Polycystin-2 expression in *orpk* mice is increased and mislocalized in intracinar dilated ducts. An acini with a severe intracinar ductal dilation is outlined in yellow. Dilated intracinar ducts (outlined in red), a structure that is not found in wild-type pancreas, show high polycystin-2 expression, comparable to levels that are only observed in intercalated ducts of control mice. Inset shows Hematoxylin/Eosin staining of a dilated intracinar duct in *orpk* mice. Cilia are also present in islets in wild-type mice (C), but are almost absent in *orpk* mice (D; arrow). Cilia are present at embryonic stages (E15.5) in wild type (E) but very few could be detected in *orpk* mice (F). Cilia length, shown in µm, is reduced in *orpk* mice (G). Tissue sections were derived from three different animals at each stage. Errors bars are shown as ±s.d. a, acini; id, intercalated duct; dd, dilated ducts.

their function appears not to be necessary for cilia formation (Hou et al., 2002; Watanabe et al., 2003).

In agreement with previous reports, and similar to *orpk* mutants (Figs 1, 3), histological and immunohistochemical analysis revealed that both *Pkd2* and inversin pancreata displayed a reduction of acinar tissue and an increase of ductular structures (Fig. 6A-H) (Morgan et al., 1998; Wu et al., 2000). As seen in *orpk* mutants, the loss of exocrine tissue in inversin mice correlates with an increase in acinar cell apoptosis (Fig. 6I,J). No increase in cell apoptosis was observed in *Pkd2* mutants (Fig. 6K,L), probably because these embryos die prematurely at E14.5. In comparison, significant levels of acinar cell apoptosis were found in *orpk* mutants only after birth. Cilia formation appeared to be unaffected in both *Pkd2* and inversin mutants as revealed by immunohistochemistry against acetylated tubulin. In addition, no increase in polycystin-2 expression was observed in inversin mutants (data not shown). These results indicate that either impairment of cilia formation in *orpk* mutants or cilia function in *Pkd2*/inversin mutant mice results in acinar cell apoptosis and ductal dilation in pancreatic tissue.

Mislocalization of β-catenin in *orpk* mice

Increasing evidence points to a crucial role of β-catenin signaling, an important regulator of cell adhesion and proliferation, during PKD formation. Previous studies showed that polycystin-1 is localized in a complex containing E-cadherin and catenins (Huan and van Adelsberg, 1999). Furthermore, transgenic mice expressing an activated mutant form of β-catenin develop PKD (Saadi-Kheddouci et al., 2001). More recently, Lin et al. have shown that kidney-specific inactivation of kinesin-II, a protein essential for cilia formation, leads to PKD with increased expression of β-catenin in epithelial kidney cells of these mice (Lin et al., 2003). We performed immunohistochemical analysis to determine whether β-catenin expression and subcellular localization is affected in *orpk* mice. Wild-type pancreatic cells exhibited a strong basolateral localization of β-catenin (Fig. 7A,C). By contrast, a substantial increase in cytoplasmic β-catenin was observed in dilated ducts of *orpk* mice (Fig. 7B,D). In addition to regulating cell adhesion via interaction with E-cadherin, β-catenin also functions as part of the Wnt signal transduction pathway. As part of this pathway β-catenin binds to Tcf/Lef transcription factors and this complex activates transcription of Wnt target genes (Nusse, 1999; Roose and Clevers, 1999; Willert and Nusse, 1998). RT-PCR was performed to determine whether the expression of these transcriptional mediators of Wnt signaling was altered in *orpk* mice. Lef1 and Tcf3 expression was increased in *orpk* mice, whereas no significant differences were found in Tcf1 and Tcf4 expression (Fig. 7E). Therefore, the polaris protein regulates intracellular localization of β-catenin and expression of Wnt signaling components in pancreatic tissue.

Discussion

Pancreatic cysts are found in about 10% of patients suffering from ADPKD (Fick et al., 1995; Torra et al., 1997). To gain insight into the mechanisms of pancreatic abnormalities observed in PKD patients, we analyzed pancreas formation and maturation in *orpk* mice.

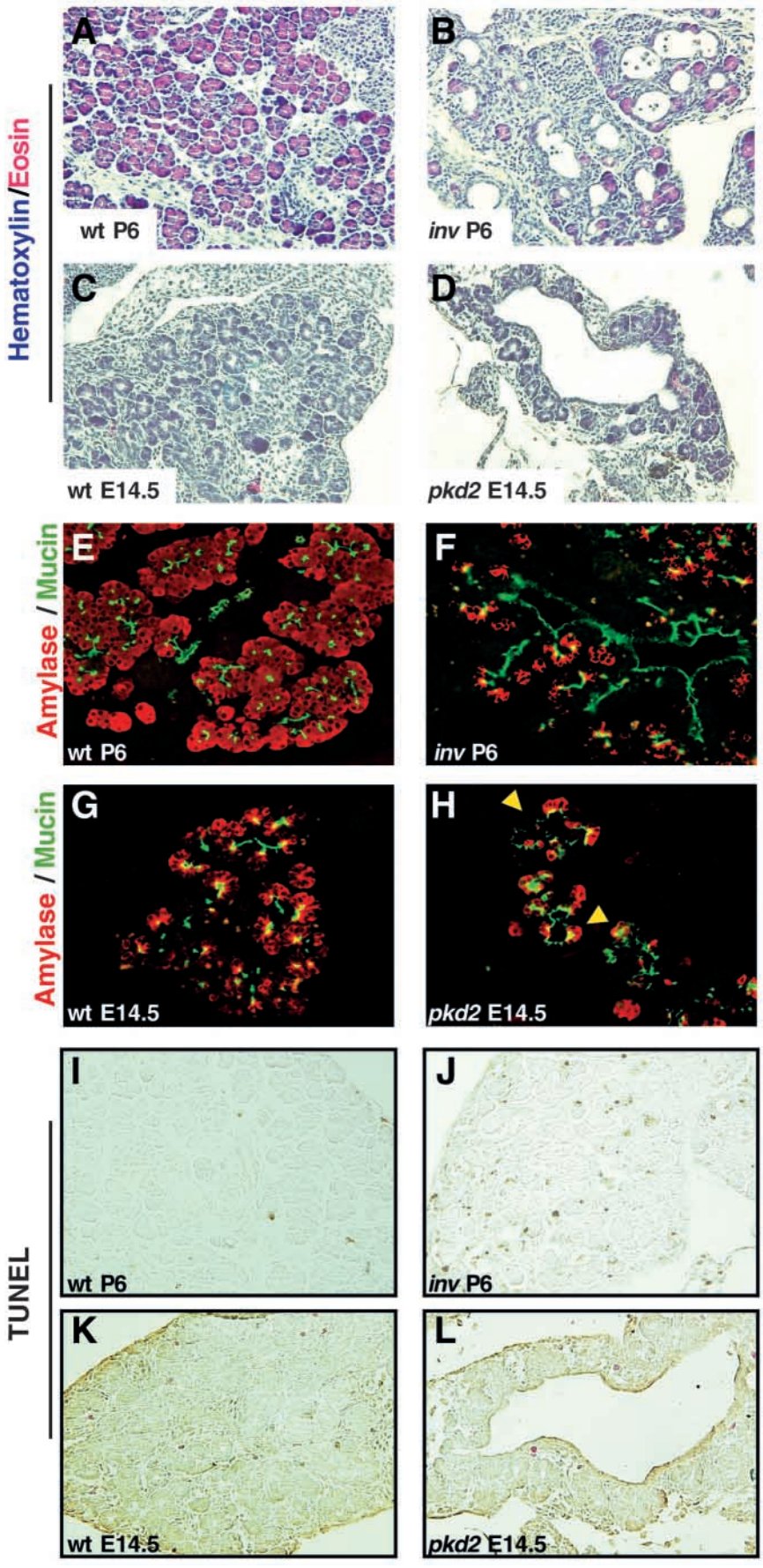

Fig. 6. Pancreatic abnormalities in inversin and *Pkd2* mice. Hematoxylin/Eosin staining of wild-type (A,C), inversin (B) and *Pkd2* mice (D), showing changes in pancreas architecture. Staining for amylase and mucin indicates normal architecture in wild-type littermates (E,G), but acinar cell loss and ductal dilation in inversin and *Pkd2* mice (F,H). Arrowheads in H indicate dilated ducts. Elevated levels of acinar cell apoptosis were observed in inversin mice (J) compared with wild-type littermates (I). No differences in apoptosis levels were detected between *Pkd2* (L) and wild-type (K) E14.5 embryos.

Pancreatic abnormalities were first detected in *orpk* mice at the end of gestation. At this time point, the intracinar ducts in *orpk* mice showed signs of dilation (Fig. 3B). The fact that defects first occur during embryonic development is consistent with the apparent reduction in cilia length at early embryonic stages (Fig. 5E-G). Dilation of pancreatic ducts becomes increasingly severe after birth, most likely caused by enhanced proliferation of the ductal epithelium (Fig. 1, Fig. 4D,F). Although the ducts are expanded, the overall size of the mutant pancreas is reduced. The decrease in pancreas size appears to be due to acinar cell atrophy, marked by increased TUNEL staining and reduced amylase expression (Figs 3, 4). The fact that an increase in acinar cell apoptosis is observed after dilation of pancreatic ducts suggests a causal relationship between these processes. Thus, two of the hallmarks of PKD, increased apoptosis and formation of tubular complexes by increased proliferation of epithelial cells, are present in pancreatic tissue in *orpk* mice.

The negligible effect of the *orpk* mutation on endocrine tissue architecture and cell differentiation is somewhat surprising considering that *Tg737* expression is highest in islets and that endocrine cells are highly ciliated (Figs 2, 5) (Aughsteen, 2001). Unfortunately, the early neonatal lethality of this line prevented us from analyzing the importance of polaris and cilia function in adult islets. Furthermore, *orpk* mice contain a hypomorphic mutation within the *Tg737* gene, and residual cilia function might mask potential defects during endocrine cell differentiation or function. At this point we can only speculate about the role of primary cilia in β-cells but an attractive hypothesis is that they also act as sensory organelles. For example, somatostatin and serotonin receptors have been found on primary cilia in neuronal cells in particular regions of the brain (Brailov et al., 2000; Handel et al., 1999). Future experiments could address whether hormone

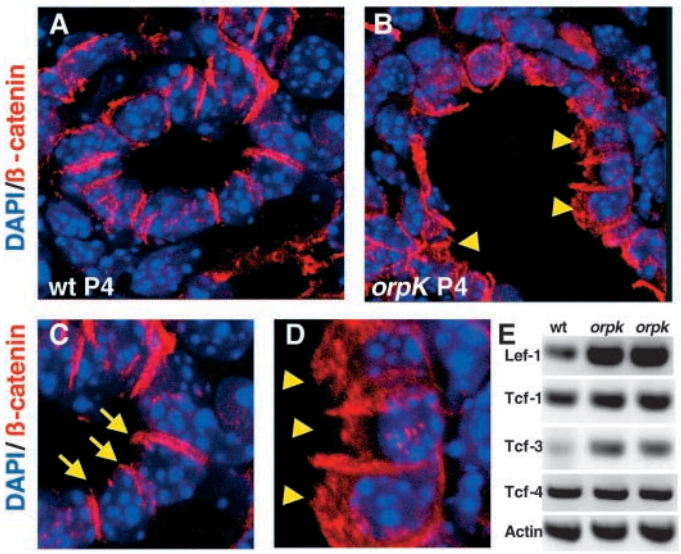

Fig. 7. Abnormal expression of β-catenin and Lef/Tcf family members in *orpk* mice. In wild-type pancreatic sections β-catenin is predominately localized to the cell membrane (A; arrows in higher magnification image, C). In *orpk* mice, cytoplasmic β-catenin localization in dilated ducts (arrowheads) is increased (B; and at higher magnification in D). (E) Expression of Lef/Tcf family members in control littermates (first lane) and *orpk* mice (second and third lane). Actin was used as a control gene.

receptors are localized on primary cilia of endocrine cells and if their activity is required to sense and respond to changes in external hormone concentration.

It is interesting to note that insulin-expressing cells were detected in *orpk* dilated ducts, thus providing support for previous studies that have described islet cell neogenesis in expanding ductal epithelium upon tissue injury (Bonner-Weir et al., 2000; Rosenberg, 1998; Wang et al., 1997). The question of whether pancreatic progenitor cells reside in ducts is still controversial (Bonner-Weir and Sharma, 2002; Gu et al., 2002), but *orpk* mice display an increased proliferation of liver oval cells, a population of cells considered to represent liver progenitor cells (Richards et al., 1996). Thus, circumstantial evidence suggests that polaris function could regulate progenitor cell proliferation in different organs.

The role of primary cilia in PKD

Tg737, the gene mutated in *orpk* mice, is required for cilia formation and several reports have recently discussed the role of cilia in various human diseases, including PKD (Pazour and Rosenbaum, 2002). Our studies show that primary cilia formation and polycystin-2 expression is altered in pancreatic cells of *orpk* mice. Cells within dilated ducts in *orpk* mice display a higher level of polycystin-2 protein, indicating that defects in cilia formation elevate cytoplasmic levels of proteins intended for delivery to the cilia. The increase in polycystin-2 expression appears to be specific to *orpk* mice as inversin mutants did not show any obvious changes in protein expression when compared with wild-type controls. The observation that inversin and *Pkd2* mice, in which cilia formation is not impaired, displayed similar pancreatic phenotypes to those found in *orpk* mice indicates that both cilia assembly and function are necessary for proper pancreas morphogenesis and maintenance of tissue architecture.

What is the normal role of primary cilia in pancreatic tissue? Recently it has been shown that cilia can act as mechanosensors to measure luminal flow (Praetorius and Spring, 2001; Praetorius and Spring, 2003), and that polycystin-1 and polycystin-2 mediate this response (Nauli et al., 2003). Cilia in pancreatic ductal cells may sense luminal pressure and control cell proliferation to maintain appropriate luminal dimensions. In the case of mutations in PKD loci (as in *Pkd2* or inversin mice), or mutations that affect ciliary assembly (as in *orpk* mice), the relay of the sensory signals that control cell division would be lost, resulting in uninhibited cell proliferation and progressive duct dilation. In agreement with this, increased pressure caused by pancreatic duct obstruction leads to ductal dilation and acinar cell death (Scoggins et al., 2000). Although speculative at this point, this hypothesis would link the similar phenotypes observed in human chronic pancreatitis, mouse models of pancreatic duct obstruction, and models with defects in primary cilia structure and function.

Cilia function regulates β-catenin localization

The exact mechanism of how defects in cilia formation and/or function cause the main manifestations of PKD is unknown. Some reports have previously suggested an involvement of β-catenin signaling in PKD (Kim et al., 1999; Saadi-Kheddouci et al., 2001). β-Catenin is involved in cell adhesion and transcriptional regulation of the Wnt signal transduction pathway (Barth et al., 1997; Polakis, 2000; Willert and Nusse, 1998). Recently, a connection between primary cilia and β-catenin signaling has been suggested. Inactivation of cilia caused by a mutation of kinesin-II leads to increased levels of cytosolic and nuclear β-catenin in renal cells (Lin et al., 2003). In agreement with those results, we observed an increase in cytoplasmic β-catenin, as well as Wnt signaling components such Lef1 and Tcf3, in pancreatic cells of *orpk* mice (Fig. 6). Thus, the pivotal role of β-catenin in regulating decisions between cell proliferation and differentiation (van de Wetering et al., 2002) is consistent with the phenotypes we have observed in *orpk* mice.

PKD, acinar-to ductal metaplasia and pancreatic adenocarcinoma

The fact that *Tg737* function is required to control intracellular localization of β-catenin, and that nuclear localized β-catenin has been found in several murine pancreatic tumors (Kongkanuntn et al., 1999), is intriguing as it provides further evidence for a previously suggested direct link between PKD and pancreatic cancer formation (Niv et al., 1997; Silverman et al., 2001). Acinar-to-ductal metaplasia, which is, at least in some cases, due to chronic pancreatitis, has been proposed as one of the mechanisms that predispose for the formation of pancreatic ductal adenocarcinomas (Malka et al., 2002). Some of the phenotypes displayed by *orpk* mice are reminiscent of those found in mouse models of pancreatic acinar-to-ductal metaplasia (Scoggins et al., 2000; Wagner et al., 1998). These features include loss of acinar cell architecture, increased ductal proliferation, stromal cell expansion and collagen deposition (Fig. 1J,K). In combination with ductal metaplasia, these defects are commonly observed in individuals suffering from chronic pancreatitis (Kloppel and Maillet, 1998) and,

to some extent, in pancreatic cancer (Kloppel, 1993). Unfortunately, due to early lethality of *orpk* mice, we were unable to test whether the lesions observed in *orpk* mice progress to neoplasia. However, mutations in the *Tg737* gene have been found in liver tumors, as well as in liver, kidney, and pancreatic human tumor cells lines, suggesting that *Tg737* functions as a tumor suppressor gene (Isfort et al., 1997). Tissue-specific and temporal inactivation of cilia components might provide evidence for a causal link between primary cilia dysfunction and pancreatic adenocarcinoma.

We thank members of the Hebrok Laboratory for helpful suggestions and stimulating discussions. We also thank Drs Michel S. German and Christian Vaisse, for discussion and sharing of experimental materials, and Drs Grace E. Kim and Yasuhiro Kosaka for histology advice. We thank Drs Paul Overbeek and Olga Cabello at Baylor College of Medicine (Houston) for the generous gift of inversin mice. We also thank Drs Stephan Somlo and Xin Tian at Yale University School of Medicine for the generous gift of *Pkd2* embryos. Work in the Hebrok Laboratory was supported by the Sandler Family Supporting Foundation, grants from the Juvenile Diabetes Research Foundation (JDRF), and an NIH grant (DK61245-01). D.A.C. was supported by a postdoctoral fellowship from the Ministerio de Educación, Cultura y Deporte of the Spanish Government. G.J.P. is supported by an NIH grant (GM-60992). N.S.M. is supported by an NIH grant (DK57306-05).

References

Ali, S. M., Wong, V. Y., Kikly, K., Fredrickson, T. A., Keller, P. M., DeWolf, W. E., Jr, Lee, D. and Brooks, D. P. (2000). Apoptosis in polycystic kidney disease: involvement of caspases. *Am. J. Physiol. Regul. Integr. Comp. Physiol.* **278**, R763-R769.

Aughsteen, A. A. (2001). The ultrastructure of primary cilia in the endocrine and excretory duct cells of the pancreas of mice and rats. *Eur. J. Morphol.* **39**, 277-283.

Barth, A. I., Nathke, I. S. and Nelson, W. J. (1997). Cadherins, catenins and APC protein: interplay between cytoskeletal complexes and signaling pathways. *Curr. Opin. Cell Biol.* **9**, 683-690.

Bonner-Weir, S. and Sharma, A. (2002). Pancreatic stem cells. *J. Pathol.* **197**, 519-526.

Bonner-Weir, S., Taneja, M., Weir, G. C., Tatarkiewicz, K., Song, K. H., Sharma, A. and O'Neil, J. J. (2000). In vitro cultivation of human islets from expanded ductal tissue. *Proc. Natl. Acad. Sci. USA* **97**, 7999-8004.

Brailov, I., Bancila, M., Brisorgueil, M. J., Miquel, M. C., Hamon, M. and Verge, D. (2000). Localization of 5-HT(6) receptors at the plasma membrane of neuronal cilia in the rat brain. *Brain Res.* **872**, 271-275.

Cai, Y., Maeda, Y., Cedzich, A., Torres, V. E., Wu, G., Hayashi, T., Mochizuki, T., Park, J. H., Witzgall, R. and Somlo, S. (1999). Identification and characterization of polycystin-2, the PKD2 gene product. *J. Biol. Chem.* **274**, 28557-28565.

Calvet, J. P. and Grantham, J. J. (2001). The genetics and physiology of polycystic kidney disease. *Semin. Nephrol.* **21**, 107-123.

Ecder, T., Melnikov, V. Y., Stanley, M., Korular, D., Lucia, M. S., Schrier, R. W. and Edelstein, C. L. (2002). Caspases, Bcl-2 proteins and apoptosis in autosomal-dominant polycystic kidney disease. *Kidney Int.* **61**, 1220-1230.

Fick, G. M., Johnson, A. M., Hammond, W. S. and Gabow, P. A. (1995). Causes of death in autosomal dominant polycystic kidney disease. *J. Am. Soc. Nephrol.* **5**, 2048-2056.

Foggensteiner, L., Bevan, A. P., Thomas, R., Coleman, N., Boulter, C., Bradley, J., Ibraghimov-Beskrovnaya, O., Klinger, K. and Sandford, R. (2000). Cellular and subcellular distribution of polycystin-2, the protein product of the PKD2 gene. *J. Am. Soc. Nephrol.* **11**, 814-827.

Gabow, P. A. (1993). Autosomal dominant polycystic kidney disease. *N. Engl. J. Med.* **329**, 332-342.

Gattone, V. H., Ricker, J. L., Trambaugh, C. M. and Klein, R. M. (2002). Multiorgan mRNA misexpression in murine autosomal recessive polycystic kidney disease. *Kidney Int.* **62**, 1560-1569.

Geng, L., Segal, Y., Peissel, B., Deng, N., Pei, Y., Carone, F., Rennke, H. G., Glucksmann-Kuis, A. M., Schneider, M. C., Ericsson, M. et al. (1996). Identification and localization of polycystin, the PKD1 gene product. *J. Clin. Invest.* **98**, 2674-2682.

Graham, R. A., Morris, J. R., Cohen, E. P. and Taylor-Papadimitriou, J. (2001). Up-regulation of MUC1 in mammary tumors generated in a double-transgenic mouse expressing human MUC1 cDNA, under the control of 1.4-kb 5′ MUC1 promoter sequence and the middle T oncogene, expressed from the MMTV promoter. *Int. J. Cancer* **92**, 382-387.

Gu, G., Dubauskaite, J. and Melton, D. A. (2002). Direct evidence for the pancreatic lineage: NGN3+ cells are islet progenitors and are distinct from duct progenitors. *Development* **129**, 2447-2457.

Handel, M., Schulz, S., Stanarius, A., Schreff, M., Erdtmann-Vourliotis, M., Schmidt, H., Wolf, G. and Hollt, V. (1999). Selective targeting of somatostatin receptor 3 to neuronal cilia. *Neuroscience* **89**, 909-926.

Hebrok, M., Kim, S. K., St Jacques, B., McMahon, A. P. and Melton, D. A. (2000). Regulation of pancreas development by hedgehog signaling. *Development* **127**, 4905-4913.

Hou, X., Mrug, M., Yoder, B. K., Lefkowitz, E. J., Kremmidiotis, G., D'Eustachio, P., Beier, D. R. and Guay-Woodford, L. M. (2002). Cystin, a novel cilia-associated protein, is disrupted in the cpk mouse model of polycystic kidney disease. *J. Clin. Invest.* **109**, 533-540.

Huan, Y. and van Adelsberg, J. (1999). Polycystin-1, the PKD1 gene product, is in a complex containing E-cadherin and the catenins. *J. Clin. Invest.* **104**, 1459-1468.

Igarashi, P. and Somlo, S. (2002). Genetics and pathogenesis of polycystic kidney disease. *J. Am. Soc. Nephrol.* **13**, 2384-2398.

Isfort, R. J., Cody, D. B., Doersen, C. J., Richards, W. G., Yoder, B. K., Wilkinson, J. E., Kier, L. D., Jirtle, R. L., Isenberg, J. S., Klounig, J. E. et al. (1997). The tetratricopeptide repeat containing Tg737 gene is a liver neoplasia tumor suppressor gene. *Oncogene* **15**, 1797-1803.

Kim, E., Arnould, T., Sellin, L. K., Benzing, T., Fan, M. J., Gruning, W., Sokol, S. Y., Drummond, I. and Walz, G. (1999). The polycystic kidney disease 1 gene product modulates Wnt signaling. *J. Biol. Chem.* **274**, 4947-4953.

Kim, S. K., Hebrok, M. and Melton, D. A. (1997). Pancreas development in the chick embryo. *Cold Spring Harb. Symp. Quant. Biol.* **62**, 377-383.

Kloppel, G. (1993). Pathology of nonendocrine pancreatic tumors. In *The pancreas: biology, pathobiology, and disease*. 2nd edn (ed. Go, V. L. W.), pp. 871-897. New York: Raven Press.

Kloppel, G. and Maillet, B. (1998). Pathology of chronic pancreatitis. In *The pancreas*, vol. 1 (ed. Sarr, M. G.), pp. 720-723. London: Blackwell Science.

Kongkanuntn, R., Bubb, V. J., Sansom, O. J., Wyllie, A. H., Harrison, D. J. and Clarke, A. R. (1999). Dysregulated expression of beta-catenin marks early neoplastic change in Apc mutant mice, but not all lesions arising in Msh2 deficient mice. *Oncogene* **18**, 7219-7225.

Lanoix, J., D'Agati, V., Szabolcs, M. and Trudel, M. (1996). Dysregulation of cellular proliferation and apoptosis mediates human autosomal dominant polycystic kidney disease (ADPKD). *Oncogene* **13**, 1153-1160.

Lin, F., Hiesberger, T., Cordes, K., Sinclair, A. M., Goldstein, L. S., Somlo, S. and Igarashi, P. (2003). Kidney-specific inactivation of the KIF3A subunit of kinesin-II inhibits renal ciliogenesis and produces polycystic kidney disease. *Proc. Natl. Acad. Sci. USA* **100**, 5286-5291.

Lu, W., Shen, X., Pavlova, A., Lakkis, M., Ward, C. J., Pritchard, L., Harris, P. C., Genest, D. R., Perez-Atayde, A. R. and Zhou, J. (2001). Comparison of Pkd1-targeted mutants reveals that loss of polycystin-1 causes cystogenesis and bone defects. *Hum. Mol. Genet.* **10**, 2385-2396.

Malka, D., Hammel, P., Maire, F., Rufat, P., Madeira, I., Pessione, F., Levy, P. and Ruszniewski, P. (2002). Risk of pancreatic adenocarcinoma in chronic pancreatitis. *Gut* **51**, 849-852.

Morgan, D., Turnpenny, L., Goodship, J., Dai, W., Majumder, K., Matthews, L., Gardner, A., Schuster, G., Vien, L., Harrison, W. et al. (1998). Inversin, a novel gene in the vertebrate left-right axis pathway, is partially deleted in the inv mouse. *Nat. Genet.* **20**, 149-156.

Moyer, J. H., Lee-Tischler, M. J., Kwon, H. Y., Schrick, J. J., Avner, E. D., Sweeney, W. E., Godfrey, V. L., Cacheiro, N. L., Wilkinson, J. E. and Woychik, R. P. (1994). Candidate gene associated with a mutation causing recessive polycystic kidney disease in mice. *Science* **264**, 1329-1333.

Murcia, N. S., Sweeney, W. E., Jr and Avner, E. D. (1999). New insights into the molecular pathophysiology of polycystic kidney disease. *Kidney Int.* **55**, 1187-1197.

Murcia, N. S., Richards, W. G., Yoder, B. K., Mucenski, M. L., Dunlap, J. R. and Woychik, R. P. (2000). The Oak Ridge Polycystic Kidney (orpk) disease gene is required for left-right axis determination. *Development* **127**, 2347-2355.

Nakanishi, K., Sweeney, W. E., Jr, Avner, E. D. and Murcia, N. S. (2001). Expression of the orpk disease gene during kidney development and maturation. *Pediatr. Nephrol.* **16**, 219-226.

Nauli, S. M., Alenghat, F. J., Luo, Y., Williams, E., Vassilev, P., Li, X., Elia, A. E., Lu, W., Brown, E. M., Quinn, S. J. et al. (2003). Polycystins 1 and 2 mediate mechanosensation in the primary cilium of kidney cells. *Nat. Genet.* **33**, 129-137.

Nauta, J., Ozawa, Y., Sweeney, W. E., Jr, Rutledge, J. C. and Avner, E. D. (1993). Renal and biliary abnormalities in a new murine model of autosomal recessive polycystic kidney disease. *Pediatr. Nephrol.* **7**, 163-172.

Niv, Y., Turani, C., Kahan, E. and Fraser, G. M. (1997). Association between pancreatic cystadenocarcinoma, malignant liver cysts, and polycystic disease of the kidney. *Gastroenterology* **112**, 2104-2107.

Nusse, R. (1999). WNT targets. Repression and activation. *Trends Genet.* **15**, 1-3.

Ong, A. C. and Wheatley, D. N. (2003). Polycystic kidney disease – the ciliary connection. *Lancet* **361**, 774-776.

Ong, A. C., Ward, C. J., Butler, R. J., Biddolph, S., Bowker, C., Torra, R., Pei, Y. and Harris, P. C. (1999). Coordinate expression of the autosomal dominant polycystic kidney disease proteins, polycystin-2 and polycystin-1, in normal and cystic tissue. *Am. J. Pathol.* **154**, 1721-1729.

Pazour, G. J. and Rosenbaum, J. L. (2002). Intraflagellar transport and cilia-dependent diseases. *Trends Cell Biol.* **12**, 551-555.

Pazour, G. J., Dickert, B. L., Vucica, Y., Seeley, E. S., Rosenbaum, J. L., Witman, G. B. and Cole, D. G. (2000). Chlamydomonas IFT88 and its mouse homologue, polycystic kidney disease gene tg737, are required for assembly of cilia and flagella. *J. Cell Biol.* **151**, 709-718.

Pazour, G. J., San Agustin, J. T., Follit, J. A., Rosenbaum, J. L. and Witman, G. B. (2002). Polycystin-2 localizes to kidney cilia and the ciliary level is elevated in orpk mice with polycystic kidney disease. *Curr. Biol.* **12**, R378-R380.

Polakis, P. (2000). Wnt signaling and cancer. *Genes Dev.* **14**, 1837-1851.

Praetorius, H. A. and Spring, K. R. (2001). Bending the MDCK cell primary cilium increases intracellular calcium. *J. Membr. Biol.* **184**, 71-79.

Praetorius, H. A. and Spring, K. R. (2003). The renal cell primary cilium functions as a flow sensor. *Curr. Opin. Nephrol. Hypertens* **12**, 517-520.

Richards, W. G., Yoder, B. K., Isfort, R. J., Detilleux, P. G., Foster, C., Neilsen, N., Woychik, R. P. and Wilkinson, J. E. (1996). Oval cell proliferation associated with the murine insertional mutation TgN737Rpw. *Am. J. Pathol.* **149**, 1919-1930.

Ricker, J. L., Gattone, V. H., 2nd, Calvet, J. P. and Rankin, C. A. (2000). Development of autosomal recessive polycystic kidney disease in BALB/c-cpk/cpk mice. *J. Am. Soc. Nephrol.* **11**, 1837-1847.

Roose, J. and Clevers, H. (1999). TCF transcription factors: molecular switches in carcinogenesis. *Biochim. Biophys. Acta* **1424**, M23-M37.

Rosenberg, L. (1998). Induction of islet cell neogenesis in the adult pancreas: the partial duct obstruction model. *Microsc. Res. Tech.* **43**, 337-346.

Saadi-Kheddouci, S., Berrebi, D., Romagnolo, B., Cluzeaud, F., Peuchmaur, M., Kahn, A., Vandewalle, A. and Perret, C. (2001). Early development of polycystic kidney disease in transgenic mice expressing an activated mutant of the beta-catenin gene. *Oncogene* **20**, 5972-5981.

Scoggins, C. R., Meszoely, I. M., Wada, M., Means, A. L., Yang, L. and Leach, S. D. (2000). p53-dependent acinar cell apoptosis triggers epithelial proliferation in duct-ligated murine pancreas. *Am. J. Physiol. Gastrointest. Liver Physiol.* **279**, G827-G836.

Silverman, J. F., Prichard, J. and Regueiro, M. D. (2001). Fine needle aspiration cytology of a pancreatic cyst in a patient with autosomal dominant polycystic kidney disease. A case report. *Acta Cytol.* **45**, 415-419.

Sorenson, C. M., Padanilam, B. J. and Hammerman, M. R. (1996). Abnormal postpartum renal development and cystogenesis in the bcl-2 (–/–) mouse. *Am. J. Physiol.* **271**, F184-F193.

Taulman, P. D., Haycraft, C. J., Balkovetz, D. F. and Yoder, B. K. (2001). Polaris, a protein involved in left-right axis patterning, localizes to basal bodies and cilia. *Mol. Biol. Cell* **12**, 589-599.

Torra, R., Nicolau, C., Badenas, C., Navarro, S., Perez, L., Estivill, X. and Darnell, A. (1997). Ultrasonographic study of pancreatic cysts in autosomal dominant polycystic kidney disease. *Clin. Nephrol.* **47**, 19-22.

Trudel, M., Lanoix, J., Barisoni, L., Blouin, M. J., Desforges, M., L'Italien, C. and D'Agati, V. (1997). C-myc-induced apoptosis in polycystic kidney disease is Bcl-2 and p53 independent. *J. Exp. Med.* **186**, 1873-1884.

van de Wetering, M., Sancho, E., Verweij, C., de Lau, W., Oving, I., Hurlstone, A., van der Horn, K., Batlle, E., Coudreuse, D., Haramis, A. P. et al. (2002). The beta-catenin/TCF-4 complex imposes a crypt progenitor phenotype on colorectal cancer cells. *Cell* **111**, 241-250.

Wagner, M., Luhrs, H., Kloppel, G., Adler, G. and Schmid, R. M. (1998). Malignant transformation of duct-like cells originating from acini in transforming growth factor transgenic mice. *Gastroenterology* **115**, 1254-1262.

Wang, R. N., Rehfeld, J. F., Nielsen, F. C. and Kloppel, G. (1997). Expression of gastrin and transforming growth factor-alpha during duct to islet cell differentiation in the pancreas of duct-ligated adult rats. *Diabetologia* **40**, 887-893.

Watanabe, D., Saijoh, Y., Nonaka, S., Sasaki, G., Ikawa, Y., Yokoyama, T. and Hamada, H. (2003). The left-right determinant Inversin is a component of node monocilia and other 9+0 cilia. *Development* **130**, 1725-1734.

Wheatley, D. N., Wang, A. M. and Strugnell, G. E. (1996). Expression of primary cilia in mammalian cells. *Cell Biol. Int.* **20**, 73-81.

Willert, K. and Nusse, R. (1998). Beta-catenin: a key mediator of Wnt signaling. *Curr. Opin. Genet. Dev.* **8**, 95-102.

Wilson, P. A. and Melton, D. A. (1994). Mesodermal patterning by an inducer gradient depends on secondary cell-cell communication. *Curr. Biol.* **4**, 676-686.

Wilson, P. D. (2001). Polycystin: new aspects of structure, function, and regulation. *J. Am. Soc. Nephrol.* **12**, 834-845.

Woo, D. (1995). Apoptosis and loss of renal tissue in polycystic kidney diseases. *N. Engl. J. Med.* **333**, 18-25.

Wu, G., Markowitz, G. S., Li, L., D'Agati, V. D., Factor, S. M., Geng, L., Tibara, S., Tuchman, J., Cai, Y., Park, J. H. et al. (2000). Cardiac defects and renal failure in mice with targeted mutations in Pkd2. *Nat. Genet.* **24**, 75-78.

Yoder, B. K., Hou, X. and Guay-Woodford, L. M. (2002a). The polycystic kidney disease proteins, polycystin-1, polycystin-2, polaris, and cystin, are co-localized in renal cilia. *J. Am. Soc. Nephrol.* **13**, 2508-2516.

Yoder, B. K., Tousson, A., Millican, L., Wu, J. H., Bugg, C. E., Jr, Schafer, J. A. and Balkovetz, D. F. (2002b). Polaris, a protein disrupted in orpk mutant mice, is required for assembly of renal cilium. *Am. J. Physiol. Renal Physiol.* **282**, F541-F552.